A Simple and Versatile Evaluation Method of Thermal Stability of NI HTS Magnets

Takanobu Mato and So Noguchi, *Member, IEEE*

***Abstract*—In this paper, a simple and versatile method of thermal stability evaluation for no-insulation (NI) high-temperature superconducting (HTS) magnets is proposed. Thermal stability is fundamental to superconducting magnets. The evaluation of coil temperature is an essential part of magnet design even though NI HTS magnets exhibit high thermal stability. Already proposed methods with complicated equivalent circuits, such as a partial element equivalent circuit (PEEC) model and a network model, require a long computation time and complication in coding. Hence, a simple way to evaluate the thermal stability of NI HTS coils is strongly desired; *e.g.*, for a preliminary-design purpose. A method proposed in the paper is a simple analytical formula derived from an equivalent RL-parallel circuit model of an NI HTS coil. The formulation considers a cooling effect with a simple assumption and Joule heating on radial (turn-to-turn contact) resistances. For a trial of the proposed simple evaluation, the thermal stability investigation is presented comparing the temperatures of the sudden discharge and ramp down. The results of the proposed analytical method are also compared with the PEEC model.**

***Index Terms*—HTS magnet, no-insulation winding technique, simple evaluation, thermal stability.**

I. Introduction

THE performances of high-temperature superconducting (HTS) magnets are increasing steadily [1]. It is attributed to the improvement of conductor performances, mechanical integrities, and magnet technologies. In particular, the no-insulation (NI) winding technique [2] plays a significant role in drastically increasing thermal stability. A key function in the NI winding technique is attributed to the capability of current sharing between turns on low-critical current regions, *i.e.*, the currents avoid the low-critical current (I_c) regions by flowing into adjacent turns through the turn-to-turn contact surfaces [3]-[6]. The current behavior of NI HTS magnets is complicated, and it is not easy to estimate the thermal stability.

The partial element equivalent circuit (PEEC) method [7]-[10] is often used to simulate the current and thermal behaviors to evaluate the thermal stability of NI HTS magnets. The PEEC method is well established, and it has demonstrated its capability of thermal stability estimation during normal operations and several scenarios such as discharge, ramp down, and normal-state transition [3], [10]-[15]. Its ability to simulate the coil behaviors is powerful in magnet research and design; however, the PEEC method has a couple of disadvantages: e.g. (1) code-implementation complexity and (2) a long computation time for large-scale magnets. When designing an NI HTS magnet as a preliminary stage, it is necessary to evaluate its thermal stability against hundreds of scenarios, such as different coil conditions, operating currents, magnetic fields, quench event cases, and so on. For the thermal estimation, a thermal simulation method (e.g. thermal finite element method) must be coupled with the complicated electric simulation method, which makes the program more complicated. We need a simple analysis method with a short calculation time but not a complicated one like the PEEC method [16].

Therefore, in the paper, we propose a simple analytical formula to estimate the thermal stability of NI HTS coils. The simple expression can be widely used in a preliminary design stage for a variety kind of magnets because of its versatility, simplicity, and very short computation time. First, the analytical coil current is formulated, followed by the coil temperature for two cases: 1) sudden discharge and 2) ramp down. The magnet de-energization scenarios after the detection of local normal zone are important for one of safe operations. To check the usage of the derivations as the first trial, the azimuthal current and the maximum temperature are analyzed for a test NI REBCO single pancake coil during sudden discharge and ramp down. An assumption of cooling effect is considered in the formulation. The analytically obtained results are validated with the PEEC method. The comparison of sudden discharge and ramp down is also presented.

II. Formulation of Current and Temperature

A. Sudden Discharge

An NI HTS coil is simply modeled with an RL circuit as

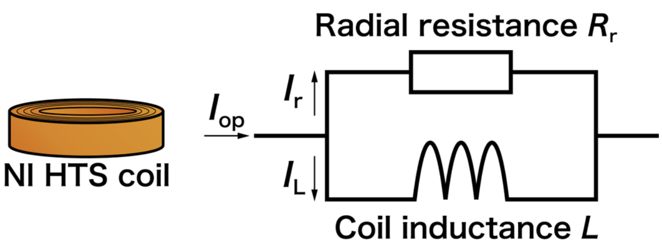

Fig. 1. NI HTS coil and its electrical equivalent circuit.

Manuscript received. This work was supported by the JSPS KAKENHI under Grant No. 22KJ0104. (Corresponding author: Takanobu Mato.)

T. Mato and S. Noguchi were with Graduate School of Information Science and Technology, Hokkaido University, Sapporo, 060-0814 Japan (e-mail: e-mail: mato@em.ist.hokudai.ac.jp, noguchi@ssi.ist.hokudai.ac.jp).

Color versions of one or more of the figures in this article are available online at http://ieeexplore.ieee.org

Digital Object Identifier will be inserted here upon acceptance.

shown in Fig. 1 [8]. The turn-to-turn (radial) resistance R_r and the coil inductance L are connected in parallel. The initial operating current of I_m flows in the azimuthal direction. Now, we derive the azimuthal current on L after the power-supply current is suddenly set to zero at $t = 0$. Here, the effect of hysteresis loss is neglected since the Joule heat on the turn-to-turn resistances are much higher [9]. The governing equation of the equivalent circuit is shown below:

$$L\frac{\mathrm{d}I_L}{\mathrm{d}t} + R_r I_r = 0 \qquad (1)$$

where I_L and I_r are the currents flowing on the coil inductance L and the contact resistance R_r, respectively. It is noted that $I_L = -I_r$ during the discharge. By solving (1) under $I_L = I_m$ at $t = 0$, we get the current exponentially decays at a speed of the time constant $\tau_e = L/R_r$:

$$I_L = I_m e^{-\frac{t}{\tau_e}}. \qquad (2)$$

Next, the temperature of the NI HTS coil is formulated. Here, it is assumed that the coil with heat capacity C is immersed in coolant of temperature T_i. The coil heat is transferred according to Fourier's law with heat transfer coefficient H [W/K]. The governing equation of coil temperature is

$$C\frac{\mathrm{d}T(t)}{\mathrm{d}t} = R_r I_r^2 - \mathrm{H}(T(t) - T_i). \qquad (3)$$

Equation (3) is solved under $T(0) = T_i$ and we get

$$T(t) = \frac{E}{C}\frac{2\tau_h}{\tau_e - 2\tau_h}\left(e^{-\frac{2t}{\tau_e}} - e^{-\frac{t}{\tau_h}}\right) + T_i. \qquad (4)$$

Note that τ_h is the time constant related to cooling, defined as C/H.

Now we may derive the time when the temperature reaches maximum temperature t_{max}. Equation (4) is differentiated and $T'(t_{max}) = 0$ is solved for t_{max}:

$$t_{max} = \frac{\ln\frac{2\tau_e}{\tau_t}}{\frac{2}{\tau_e} - \frac{1}{\tau_h}}. \qquad (5)$$

Looking at (4), the time-transient temperature is defined with the sum of two exponentials with different time constants: $\tau_e/2$ and τ_h. The balance of the cooling timescale and Joule heat timescale determines the temperature rise as well as the maximum temperature. The contact resistance R_r changes the electrical time constant τ_e, and it would non-linearly affect the thermal stability, as mentioned later.

B. Ramp down

The current and the temperature during ramp down are derived in this section. Fig. 2 shows an operating current pattern. The operating current I_{op} decays at a constant rate of r [A/s] from I_m, defined as the following equation:

$$I_{op} = \begin{cases} I_m - rt & (0 \le t < t_0) \\ 0 & (t_0 < t) \end{cases}. \qquad (6)$$

It is noted that $I_L = I_{op} - I_r$. The governing equation of current is the same as (1), and we get the analytical solutions:

$$I_L = \begin{cases} r\tau_e\left(1 - e^{-\frac{t}{\tau_e}}\right) + I_{op} & (0 \le t < t_0) \\ r\tau_e\left(e^{-\frac{t-t_0}{\tau_e}} - e^{-\frac{t}{\tau_e}}\right) & (t_0 < t) \end{cases} \qquad (7)$$

$$I_r = \begin{cases} -r\tau_e\left(1 - e^{-\frac{t}{\tau_e}}\right) & (0 \le t < t_0) \\ -r\tau_e\left(e^{-\frac{t-t_0}{\tau_e}} - e^{-\frac{t}{\tau_e}}\right) & (t_0 < t) \end{cases}. \qquad (8)$$

The radial current exponentially changes, and its maximum is determined with the ramp-down rate and the electrical time constant. A large contact resistance and a slow ramp-down rate prevent the coil from large Joule heating on the contact resistance. Incidentally, the formulation of the current behavior for ramp up to charge NI HTS pancake coils, found in [17], is similar to (7), (8).

By substituting (8) into (3) and solving it, we get the temperature expression:

$$T(t) = \begin{cases} f(t) - f(0)e^{-\frac{t}{\tau_h}} + T_i & (0 \le t < t_0) \\ g(t) + \left(f(t_0) - g(t_0)\right)e^{-\frac{t-t_0}{\tau_h}} \\ \qquad -f(0)e^{-\frac{t}{\tau_h}} + T_i. & (t_0 < t) \end{cases} \qquad (9)$$

The functions $f(t)$ are given as

$$f(t) = \frac{R}{H}r^2\tau_e^2\left(1 - \frac{2\tau_e}{\tau_e - \tau_h}e^{-\frac{t}{\tau_e}} + \frac{\tau_e}{\tau_e - 2\tau_h}e^{-\frac{2t}{\tau_e}}\right) \qquad (10)$$

$$g(t) = \frac{R}{H}\frac{\tau_e}{\tau_e - 2\tau_h}I_r^2. \qquad (11)$$

Similarly, t_{max} is derived by solving $T'(t) = 0$ in $t_0 < t$:

$$t_{max} = \frac{\ln\frac{B}{A}}{\frac{2}{\tau_e} - \frac{1}{\tau_h}} \qquad (12)$$

where

$$A = f(0) - \left(f(t_0) - g(t_0)\right)e^{\frac{t_0}{\tau_h}}$$

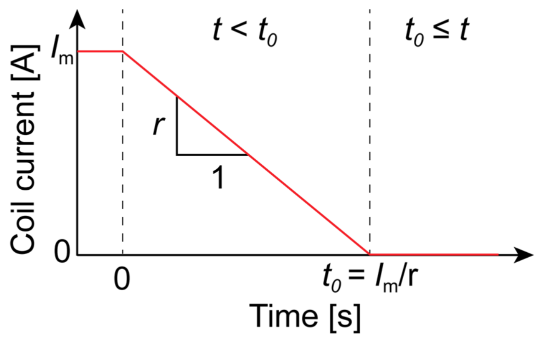

Fig. 2. Operating current pattern for ramp down discharging.

TABLE I
COIL SPECIFICATIONS AND OPERATION PARAMETERS

Parameters	Values
I.D.; O.D.; Height [mm]	50, 90, 4.0
Number of turns	200
Number of single pancakes	1
Initial operating current [A]	268.6
Coolant temperature [K]	4.2
Magnetic field [T]	7 (background 5 T)
Stored energy [J]	125
Magnet heat capacity [J/K]	15.8
Heat transfer coefficient [W/(K·m^2)]	100
Ramp down rate [A/s]	1, 10, 100, 1000

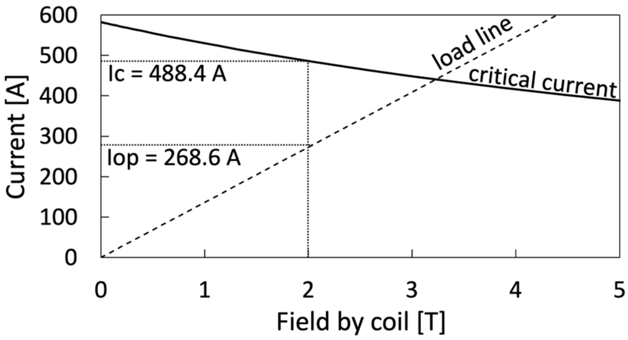

Fig. 3. Critical current and load line of investigated NI HTS coil.

$$B = \frac{R}{H}\frac{2\tau_{\mathrm{h}}}{\tau_{\mathrm{e}} - 2\tau_{\mathrm{h}}} r^2 \tau_{\mathrm{e}}^2 \left(e^{\frac{t_0}{\tau_{\mathrm{e}}}} - 1\right)^2.$$

For both cases of sudden discharge and ramp down, the thermal stability can be easily investigated with the maximum temperature $T_{\max} = T(t_{\max})$.

III. Thermal Stability Investigation

As explained above, we derived the formula of the analytical coil current and the analytical temperature. We tested these formulas applying to an arbitrary NI HTS single pancake coil. The specifications of the NI HTS single pancake coil investigated are listed in Table I. The single pancake coil is wound with REBCO tapes with 200 turns. It generates 2 T with the operating current I_{op} = 268.6 A under a background field of 5 T. A critical current and a load line of the NI REBCO coil are shown in Fig. 3. The critical current model in [18] is used. The operating current is 268.6 A at the initial state. It is assumed that the NI REBCO coil is immersed with liquid helium, cooled through the coil surfaces. Here, the heat transfer coefficient of 100 W·K^{-1}·m^{-2} is used as a constant, referred from [19].

A. Thermal stability with different contact resistances

First, the decaying currents and temperatures are analyzed in both cases of sudden discharge and ramp down, with the different contact resistivities of 0.07, 0.7, and 7 mΩ·cm^2, which corresponds to the contact resistances of 1.63, 16.3, and 163 mΩ, respectively. Fig. 4 shows the azimuthal current by (2) and the radial one, and the coil temperature obtained from (4) in the case of sudden discharge. The Joule heat is also shown in Fig. 4. Once the NI REBCO pancake coil is shut off from the power source at t = 0, the azimuthal current exponentially decays. In the case of high contact resistance, the current decay speed is fast. The Joule heat is very high at the beginning of shutting-off, and then it immediately drops to zero. Contrarily, in the case of low contact resistance, the Joule heat occurs for a long time.

Using (4), the temperature transient is easily analyzed as shown in Fig. 4. The coil temperature slowly increases in the case of 0.07 mΩ·cm^2 due to the slow decaying speed of the current, exhibiting the slow decrease by cooling. In the case of the higher contact resistance, the coil temperatures steeply increase, and its maximums are higher than 0.07 mΩ·cm^2. The thermal behaviors are easily and simply clarified using the analytical solution.

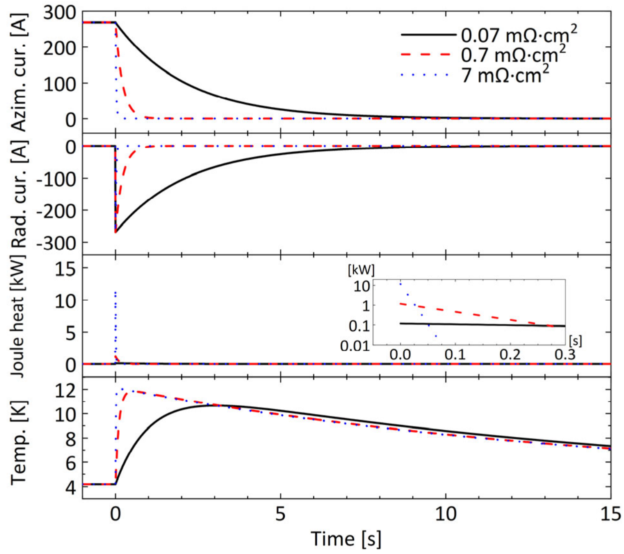

Fig. 4. Azimuthal current, radial current, and coil temperature in case of sudden discharge.

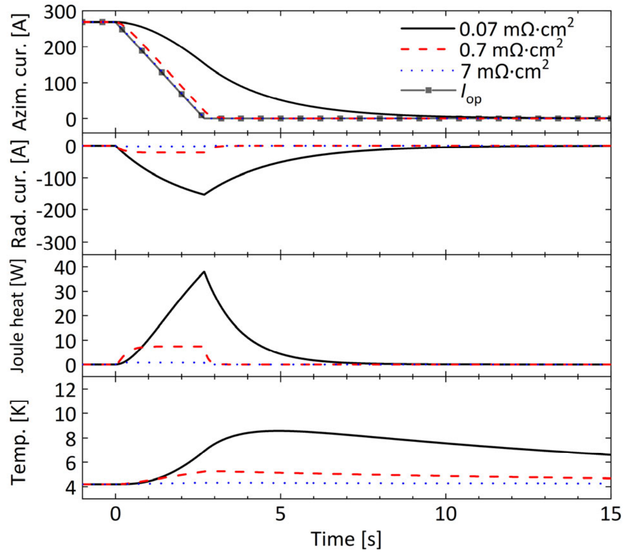

Fig. 5. Azimuthal current, radial current, and coil temperature in case of ramp down.

Fig. 5 is the case of ramp down analyzed with (7) for the azimuthal current, (8) for the radial current, and (9) for the coil temperature. The azimuthal current is almost identical to the operating current in the case of 7 mΩ·cm^2; meanwhile, the azimuthal current decays in long time at 0.07 mΩ·cm^2. The radial current gradually decreases down to the value defined with $r\tau_{\mathrm{e}}$, and then it is back to zero. Almost zero radial current flows when the contact resistance is high. The high contact resistance obviously prevents the current from flowing in a radial direction. Meanwhile, the low contact resistance allows the current to flow in the radial direction. The large radial current results in the generation of large Joule heat in the NI REBCO pancake coil for a long time. The radial current increases until $t = t_0$, maintaining generating the large Joule heat. Even after t_0, the pancake coil is heated up due to the long decay time of the radial current.

From the above current behaviors, it is obvious that the high contact resistance results in lower temperature rise. The lower the contact resistivity is, the higher the maximum temperature is. It is the opposite tendency to the sudden discharge.

The above-mentioned behaviors are commonly seen in NI pancake coils. The presented formulations are sufficient to preliminarily evaluate the thermal stability. It is possible to roughly but easily estimate the temperature rise and the maximum temperature in ideal cases.

B. Comparison of sudden discharge and ramp down

The maximum temperatures are compared in the cases of sudden discharge and ramp down. Fig. 6 plots the maximum temperature as a function of the turn-to-turn contact resistance (the radial turn-to-turn contact resistance) obtained from the simple formula and the radially divided PEEC method using the same thermal condition [20]. The result from the proposed simple method and the PEEC method obviously agree well. The validation of the proposed analytical method is confirmed.

For the sudden discharge, the maximum temperature monotonously increases with the contact resistivity, because the NI HTS coil is rapidly heated up due to the large Joule heating after the sudden discharge.

Whereas, for ramp down, not only the contact resistivity but also the ramp-down rate determines the maximum temperature. The slow ramp-down rates result in low maximum temperatures at an arbitrary contact resistance because a low voltage is induced and the radial leakage current through the turn-to-turn surface is small. The maximum temperature decreases as the contact resistance increases further. That is, a small radial current carries due to the high contact resistance. The low maximum temperature at the low contact resistivity is caused by the cooling effect because the cooling effectively appears due to the slow ramp-down rate. Here, Fig. 7 is the maximum temperature like Fig. 6, but with an adiabatic thermal condition. The maximum temperature monotonously decreases as the contact resistance increases. It is clearly shown that the cooling effect significantly affects the maximum temperature rise in the low contact resistance region from a comparison of Figs. 6 and 7.

When the contact resistance is high to prevent the charging delay, the ramp-down rate should be slow for any cooling condition to achieve high thermal stability, but not sudden discharge.

III. Conclusion

In this paper, we presented the simple expressions of temperature in case of sudden discharge and ramp down. The simple expressions can be used easily in a preliminary design stage. It takes a very short computation time.

In addition, the thermal stabilities are compared between sudden discharge and ramp down. The comparison results show that the ramp down is better than sudden discharge from the viewpoint of maximum temperature, proving that sudden discharge is the worst case to de-energize magnets. The effects of ramp down speed and contact resistances on maximum temperature are investigated as well. The lower the ramp down rate is, the higher the thermal stability is. In terms of resistance, the high contact resistance results in low-temperature rise because the high contact resistance prevents current from flowing in turn-to-turn contact resistances. The NI HTS coil with very low contact resistance also showed high thermal stability because the magnetic stored energy is dissipated gradually for a long time. Meanwhile, the NI HTS coil must be cooled sufficiently.

The simple expression presented in this paper is for the target of a preliminary evaluation. The calculations for all the cases in this paper took less than 2 s in total, therefore it is clear evidence for its simplicity, while it maintains the accuracy. Since the electromagnetic phenomenon and the cooling effect are much more complicated, precise behavior simulation is desired for a final design stage with a sophisticated simulation method such as the partial element equivalent circuit or the network model with a thermal simulation.

In the proposed formulation, HTS resistances due to local normal zones are not taken into account. The consideration of local-normal-zone or fully-normal-transition resistance is a future task. Furthermore, the stability of HTS coils during enegization will also be formulated analytically.

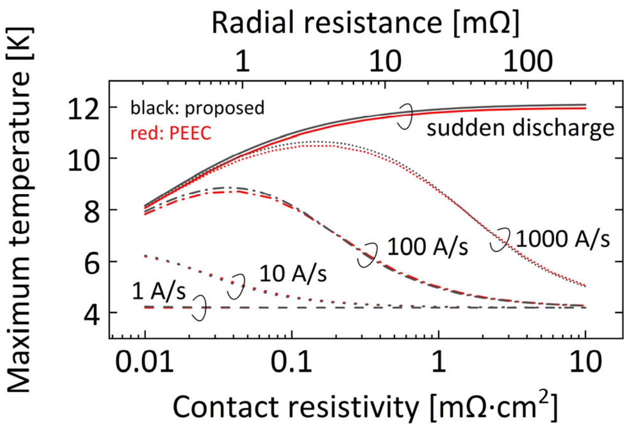

Fig. 6. Maximum temperature as a function of contact resistivity with cooling effect. Black lines show the results of the simple estimation formula. Red ones are calculated with the PEEC method.

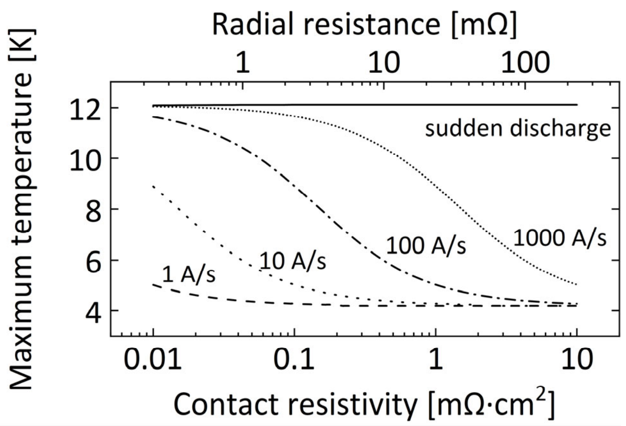

Fig. 7. Maximum temperature as a function of contact resistivity with adiabatic condition.

REFERENCES

[1] H. Maeda and Y. Yanagisawa, “Future prospects for NMR magnets: A perspective,” *J. Magn. Reson.*, vol. 306, pp. 80–85, 2019.

[2] S. Hahn, D. K. Park, J. Bascuñán, and Y. Iwasa, “HTS Pancake Coils without Turn-to-Turn Insulation,” *IEEE Trans. Appl. Supercond*., vol. 21, no. 3, pp. 1592–1595, 2011.

[3] A. Ikeda et al., “Transient Behaviors of No-Insulation REBCO Pancake Coil During Local Normal-State Transition,” *IEEE Trans. Appl. Supercond*., vol. 26, no. 4, 2016, Art. no. 4600204.

[4] T. Oki et al., “Evaluation on Quench Protection for No-Insulation REBCO Pancake Coil,” *IEEE Trans. Appl. Supercond*., vol. 26, no. 4, 2016, Art. no. 4702905.

[5] W. Denis Markiewicz, T. Painter, I. Dixon, and M. Bird, “Quench Transient Current and Quench Propagation Limit in Pancake Wound REBCO Coils as a Function of Contact Resistance, Critical Current, and Coil Size,” *Supercond. Sci. Technol*., vol. 32, no. 10, 2019, Art. no. 105010.

[6] A. V. Gavrilin, D. J. Kolb-Bond, K. L. Kim, K. Kim, W. S. Marshall, and I. R. Dixon, “Quench and Stability Modelling of a Metal-Insulation Multi-Double-Pancake High-Temperature-Superconducting Coil,” *IEEE Trans. Appl. Supercond.*, vol. 31, no. 5, 2021, Art. no. 4601707.

[7] A. E. Ruehli, “Equivalent Circuit Models for Three-Dimensional Multiconductor Systems,” *IEEE Trans. Microw. Theory Tech*., vol. 22, no. 3, pp. 216–221, 1974.

[8] S. Noguchi, “Electromagnetic, Thermal, and Mechanical Quench Simulation of NI REBCO Pancake Coils for High Magnetic Field Generation,” *IEEE Trans. Appl. Supercond*., vol. 29, no. 5, Aug. 2019, Art. no. 4602607.

[9] K. Daiho, A. Ishiyama, and S. Noguchi, “AC Loss Evaluation of NI REBCO Pancake Coils in External Low-Frequency Magnetic Field,” *IEEE Trans. Appl. Supercond.*, vol. 32, no. 6, 2022, Art. no. 5901305.

[10] X. Wang, T. Wang, E. Nakada, A. Ishiyama, R. Itoh, and S. Noguchi, “Charging Behavior in No-Insulation REBCO Pancake Coils,” *IEEE Trans. Appl. Supercond*., vol. 25, no. 3, 2015, Art. no. 4601805.

[11] T. Mato, R. Inoue, H. Ueda, S. Kim, and S. Noguchi, “Investigation into Accuracy of Turn-To-Turn Contact Resistance Measurement in Low-Frequency AC Method by 3D Numerical Simulation,” *Supercond. Sci. Technol*., vol. 36, no. 1, 2022, Art. no. 014005.

[12] D. Liu, H. Yong, and Y. Zhou, “Analysis of Charging and Sudden-Discharging Characteristics of No-Insulation REBCO Coil Using an Electromagnetic Coupling Model,” *AIP Adv*., vol. 7, no. 11, 2017, Art. no. 115104.

[13] D. Liu, W. Zhang, H. Yong, and Y. Zhou, “Thermal Stability and Mechanical Behavior in No-Insulation High-Temperature Superconducting Pancake Coils,” *Supercond. Sci. Technol.*, vol. 31, no. 8, 2018, Art. no. 085010.

[14] Y. Wang, W. K. Chan, and J. Schwartz, “Self-Protection Mechanisms in No-Insulation (RE)Ba2Cu3Ox High Temperature Superconductor Pancake Coils,” *Supercond. Sci. Technol.*, vol. 29, no. 4, 2016, Art. no. 045007.

[15] D. Liu, D. Li, W. Zhang, H. Yong, and Y. Zhou, “Electromagnetic-Thermal-Mechanical Behaviors of a No-Insulation Double-Pancake Coil Induced by a Quench in The Self Field and The High Field,” *Supercond. Sci. Technol.*, vol. 34, no. 2, 2021, Art. no. 025014.

[16] S. Noguchi, S. Hahn, A. Ishiyama, and Y. Iwasa, “A Simple Protection Evaluation Method for No-Insulation REBCO Pancake Coils during Local Normal-State Transition,” *Supercond. Sci. Technol.*, vol. 32, no. 4, 2019, Art. no. 045001.

[17] Y. Wang, H. Song, W. Yuan, Z. Jin, and Z. Hong, “Ramping Turn-to-Turn Loss and Magnetization Loss of a No-Insulation (RE)$Ba_2Cu_3O_x$ High Temperature Superconductor Pancake Coil,” *J. Appl. Phys.*, vol. 121, no. 11, 2017, Art. no. 113903.

[18] H. Ueda et al., “Numerical Simulation on Magnetic Field Generated by Screening Current in 10-T-Class REBCO Coil,” *IEEE Trans. Appl. Supercond*., vol. 26, no. 4, 2016, Art. no. 4701205.

[19] Y. Iwasa, “Stability,” in *Superconducting Magnets: Design and Operational Issues*, 2nd ed. NY, USA: Springer Science+Business Media, 2009, ch. 8, sec. 6, pp. 359.

[20] S. Noguchi, “Electromagnetic, Thermal, and Mechanical Quench Simulation of NI REBCO Pancake Coils for High Magnetic Field Generation,” *IEEE Trans. Appl. Supercond.*, vol. 29, no. 5, 2019, Art. no. 4602607.